A SIMPLE METHOD FOR ANALYZING THE DYNAMIC BEHAVIOUR OF INDUCTION MOTOR DRIVES CONTROLLED BY CURRENT SOURCE INVERTER

By

J. LÁZÁR

Department of Electric Machines, Technical University, Budapest
Received February 25, 1977
Presented by Prof. Dr. Gy. Retter

1. Introduction

Fig. 1 shows the known general shematic of an ac-motor drive controlled by a Current Source Inverter (CSI). The exact analysis of the dynamic performance of such a drive-system is not a simple problem because of the many energy storages and many types of current conducting conditions. An exact analysis can be carried out by analogue simulation or by using a digital computer, but these methods are suitable rather for the control of an already planned system, than for planning. Therefore, in practical planning all the approximation methods are very significant which, though by simplifications, make possible a faster survey of the machine performance in whole ranges of the most important parameters. Dimensioning of the main elements of the system is also possible on this basis.

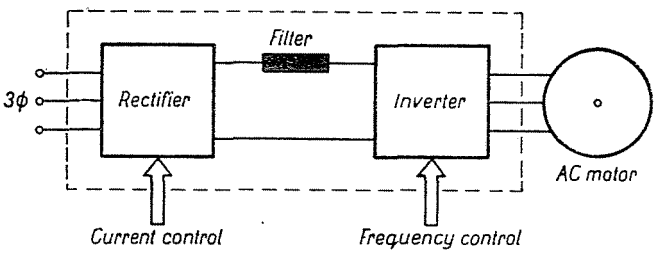

Fig. 1. Principled schematic of an induction motor drive controlled by a Current Source Inverter

For analyzing the dynamical performance, approximation methods can be found in the literature (see [2]). A general feature of the approximation methods is that in the machine they neglect the higher harmonics and consider only the fundamental frequency quantities. A comparison of the results obtained by such a method and by the exact one shows that, practically in most cases, this approximation is justified; it will be adopted here, too. The next and most important approximation is that only one current conduction mode out of the known three modes occurring in the operational process of the CSI-system, i.e. the purely two-phase conducting

state, will be considered, while the commutation of the current and the preceding charging process of the commutating capacitors will be neglected. In this way the system—even with considering the filter-choke—will be simplified to a four-energy-storage system (a mechanical, two rotor and one stator time constant) instead of the original nine-energy-storage systems.

The present paper makes a further step in approximating the inverter and applies a somewhat rougher approximation. It was assumed that, if the commutation process of the inverter is neglected, then compared with this, the assumption of the basic feature of the system, namely that feeding by CSI means practically a current force, to be perfect will not cause an unacceptable rough error. On this basis the real CSI is replaced by an idealized current source, as shown in Fig. 2.

This Ideal Current Source (ICS) forces on the stator windings of the motor a symmetrical three-phase fundamental frequency current, whose amplitude and frequency can be changed continuously in the desired interval. The internal resistance of the ICS is infinitely great, the stator current determined in the opened loop or by a regulator will set in without time-delay. Thus the time-constants or energy storages of the stator are neglected by this approximation; neglection of the higher harmonics is a usual approximation.

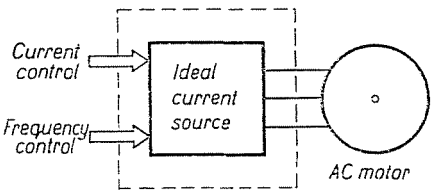

Fig. 2. Approximation of a CSI-drive with Ideal Current Source

With the assumption made above we have a mathematical model containing three energy storages; in the following an application of this model will be presented. At first sight the neglection of the stator time constants may seem to be a very rough approximation. However, it must be considered that the stator time constant in the more exact approximation (with four storages) derives from the stator inductances which — as a consequence of the current source character — play a smaller role, e.g., from the view-point of stability than the commutating capacitors do, which are neglected in every approximation method. Thus it could rather be said that, compared with the neglection of the capacitors, all the other neglections on the stator side are only of secondary importance. Anyhow, when applying an approximative method in planning the system, the operational points which seem to be critical must always be checked by one of the exact methods.

2. Equivalent circuit, basic equations

The equations of induction motors are nonlinear, therefore we examine the small deviations around the static operating point in the known way, and linear equations will be obtained. The following method is similar to that in section 8 of [3]. Let $\bar{I}$ be the stator current caused by the ICS in a given operating point, and W_1 the synchronous speed determined by the stator frequency. Let us use the Park-vectors for describing the electromagnetic quantities [5]. It is practicable to work in a coordinate system rotating at the synchronous W_1 of the given operating point, as here the operating point parameters are constant. We assume the stator current in the operating point to lie in the direction of the real axis, therefore $\bar{I}=I$ (Fig. 3).

Let the small deviation of the current amplitude be Δi. If the frequency, too, changes at the same time, the current Park-vector will turn by a small angle φ, and the new current will be $\bar{\imath}=(I+\Delta i)e^{j\varphi}$. The resulting small deviation of the stator current is therefore: $\Delta\bar{\imath}_s=\bar{\imath}-I$. In the following, small deviations are indicated by small letters without Δ, and the parameters in the operational point and other constants by capital letters. Neglecting the secondary small quantities, one can write

$$\bar{\imath}_s=I(a+j\varphi) \tag{1}$$

Here $a=\Delta i/I$ is the relative change of the amplitude. The small deviation of the synchronous speed is:

$$w_1=\frac{\mathrm{d}\varphi}{\mathrm{d}t}=s\varphi \tag{2}$$

where s is the variable of the Laplace transformation.

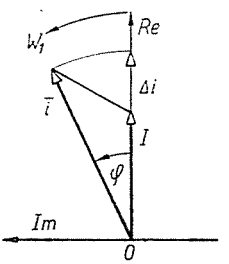

Fig. 3. Vector diagram of stator current for small deviations

By application of the reduction factor $\mu=L_m/L_r$, the rotor parameters can be reduced to the stator side in such a way, that the stray inductance of the rotor will disappear; the reduced rotor flux is $\bar{\psi}_r^*=\mu\bar{\psi}_r$, the rotor current $\bar{\imath}_r^*=\bar{\imath}_r/\mu$ and the resistance $R_r^*=\mu^2R_r$. After reduction, an equivalent circuit valid for the fluxes and currents is derived as shown in Fig. 4/a, which holds both for transient and for steady-

state conditions. (It is not necessary to explain in more detail the symbols, as they are in accordance with the international literature.) From the equivalent circuit:

$$\bar{\psi}_r^* = (L_s - L_s')(\bar{i}_s + \bar{i}_r^*), \tag{3}$$

which holds for small and great deviations alike.

As the ICS directly determines the stator current, it is sufficient to write the rotor voltage equation. Assuming great deviations for the time being, one can write in the chosen coordinate system:

$$\bar{i}_r^* R_r^* + \frac{\mathrm{d}\bar{\psi}_r^*}{\mathrm{d}t} + j(W_1 - W)\bar{\psi}_r^* = 0. \tag{4}$$

Here W is the speed of the rotor. Equations (3) and (4), in steady-state conditions follow from the equivalent circuit of Fig. 4/b. From this, the rotor flux in a static operating point:

$$\bar{\Psi}_r^* = \frac{(L_s - L_s')I}{1 + j(W_1 - W)T_r} \tag{5}$$

where $T_r = L_r/R_r$ is the time constant of the rotor.

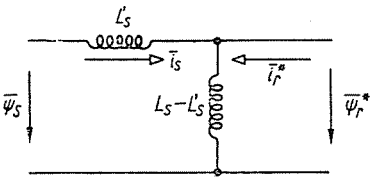

Fig. 4/a. Equivalent circuit of induction motor for the fluxes and currents

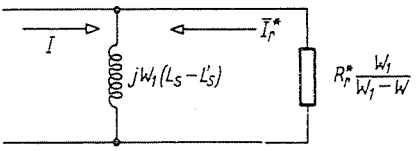

Fig. 4/b. Steady state equivalent circuit

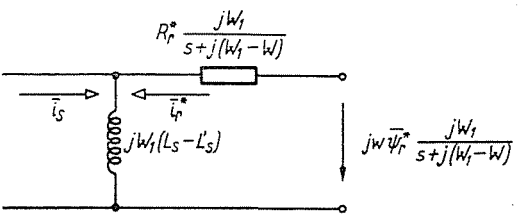

Fig. 4/c. Transient equivalent circuit for small deviations

In the following we use the per-unit system, using the nominal values of the motor as fundamental units. In this system $1/T_r = S_b$ is equal to the breakdown slip of the motor supplyed by ICS, so

$$(W_1 - W)T_r = \frac{S}{S_b} = \sigma \tag{6}$$

means the actual slip related to the breakdown slip. With this

$$\bar{\Psi}_r^* = \frac{L_s - L_s'}{1 + j\sigma} I \tag{5a}$$

and the amplitude:

$$\Psi_r^* = \frac{L_s - L_s'}{\sqrt{1+\sigma^2}} I. \tag{5b}$$

Finally the electromagnetic torque of the motor in a static operating point:

$$M = \bar{\Psi}_r^* \times I = \mathrm{Re}\,[-j\bar{\psi}_r^* I] = (L_s - L_s')I^2 \frac{\sigma}{1+\sigma^2}. \tag{7}$$

(The circumflex means a conjugate.)

In transient the speed of the motor also varies, so eq. (4) will not be linear; by changing over to small deviations and the Laplace-transformation, the linearized voltage equation of the rotor will be:

$$\bar{i}_r^* R_r^* + [s + j(W_1 - W)]\bar{\psi}_r^* - jw\bar{\Psi}_r^* = 0 \tag{8}$$

From eq. (3) and (8) we get the equivalent circuit of Fig. 4/c; this is valid in the transient states for small deviations.

It is practicable to introduce the operator inductance of the rotor, with using (6) this will be

$$\bar{l}_r(s) = \frac{L_s - L_s'}{1 + sT_r + j\sigma}. \tag{9}$$

With this, or by using the equivalent circuit or the equations, the deviation of the rotor flux in the vicinity of an operational point:

$$\bar{\psi}_r^* = \bar{l}_r \bar{i}_s + jwT_r \frac{\bar{\Psi}_r^*}{L_s - L_s'} l_r. \tag{10}$$

The small deviation of the torque:

$$m = \bar{\psi}_r^* \times I + \bar{\Psi}_r^* \times \bar{i}_s = \bar{\Psi}_r^* \times \bar{i}_s - I \times \bar{\psi}_r^* = \mathrm{Re}\,[-j\hat{\Psi}_r^* \bar{i}_s + jI\bar{\psi}_r^*] \tag{11}$$

Finally, the mechanical equation of motion in the p.u. system, for small deviations:

$$m - m_L = sT_{SN} w \tag{12}$$

where m_L is the small deviation of load torque, and T_{SN} is the nominal starting time of the drive. In the following we assume that the load torque is not dependent on the speed in the small vicinity of the operating point.

3. Transfer functions, block diagram

Substituting the rotor flux (10) into the expression of the torque (11):

$$m=\mathrm{Re}\left[(j\bar{I}_r-j\hat{\Psi}_r^*)\bar{i}_s-wT_r\bar{I}_r\frac{\bar{\Psi}_r^*}{L_s-L_s'}\right]. \tag{13}$$

Using this expression, the equation of motion (12) and formula (1), the block diagram shown in Fig. 5 can be drawn. In this block diagram the element "Re" is unusual which refers to the forming of the real part necessary in the torque equation. A block diagram which can be used in practice can obviously be derived by expressing in detail this element.

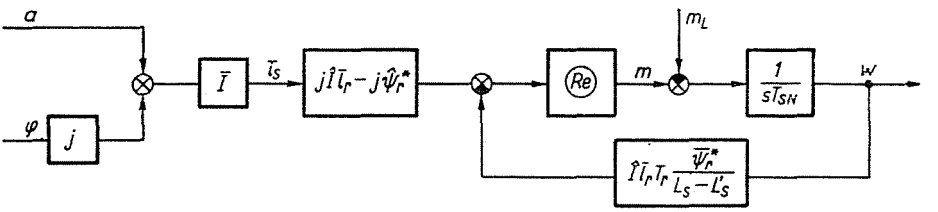

Fig. 5. Block diagram for small deviations

From the block diagram and Eq. (13) it can be seen, that the small deviation of the torque arises as a consequence of the input-signals a and φ and the change of speed w. Because of linearity, the superposition principle holds, therefore the small deviation of the torque — caused by the signals mentioned — can be expressed as:

$$m=Y_{ma}a+Y_{m\varphi}\varphi+Y_{mw}w \tag{14}$$

where Y_{ma}, $Y_{m\varphi}$, and Y_{mw} are the transfer functions of the torque relative to each of the input-signals, if in the case of an input-signal the other two are zero. From (13), considering (1),

$$Y_{ma}=\left[\frac{m}{a}\right]_{\substack{\varphi=0\\w=0}}=I\,\mathrm{Re}\,[j\bar{I}_r+j\bar{\Psi}_r^*] \tag{15a}$$

$$Y_{m\varphi}=\left[\frac{m}{\varphi}\right]_{\substack{a=0\\w=0}}=-I\,\mathrm{Re}\,[\bar{I}_r-\bar{\Psi}_r^*] \tag{15b}$$

$$Y_{mw}=\left[\frac{m}{w}\right]_{\substack{a=0\\\varphi=0}}=-\frac{IT_r}{L_s-L_s'}\,\mathrm{Re}\,[\bar{I}_r\bar{\Psi}_r^*] \tag{15c}$$

where the variable s can be regarded as real when forming the real part. The denominators of all of the transfer functions as s- functions are the same, and are of second order for s; the two roots are the conjugates of each other, as the denominator is obtained as the product of the denominator of the operator inductance and its conjugate, while forming the real part. So the poles of the transfer functions can directly be expressed by using the first-order denominator of (9):

$$p_{1,2}=-\frac{1}{T_r}\pm j(W_1-W). \tag{16}$$

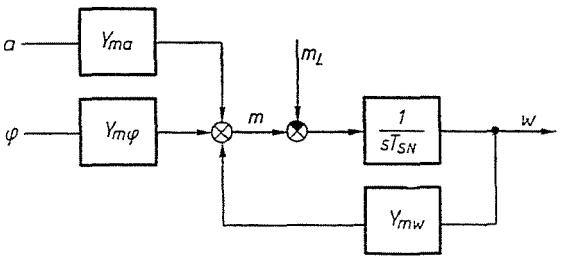

Fig. 6. Block diagram with real transfer functions

As a result we obtain the block diagram fo Fig. 6 with the transfer functions defined above. From this the dynamical performance of the drive can be studied, if the input-signals are the current-amplitude, the frequency or their arbitrary combination, and the load torque. To the analyses any method known from control theory can be applied.

4. The stability criterion of the uncontrolled system

For the purpose of presenting the application of the foregoing transfer function and block diagram let us first examine briefly the question of stability in the case of an uncontrolled system. Here it is practicable to use the root-locus method. If there is no control of any kind, then $a=0$ and $\varphi=0$, and so the effect of changing the load torque upon the speed or the torque of the motor can be studied. From the block diagram of Fig. 6 for the uncontrolled case only the right-hand — from w to Y_{mw} — feedback part will remain, where the resultant transfer function of the opened loop is:

$$Y_0=-\frac{1}{sT_{SN}}Y_{mw}.$$

Here, using the expression (15c) of Y_{mw}, with the symbols already introduced, we get:

$$Y_0=\frac{I^2(L_s-L_s')T_r}{1+\sigma^2}\,\frac{1+sT_r-\sigma^2}{sT_{SN}(1+sT_r+j\sigma)(1+sT_r-j\sigma)}.$$

The two poles of this transfer function were expressed in (16), the third one is $p_3=0$. The root-loci representing the roots of the characteristic equation of the closed-loop system start from the poles and run either to the infinite or to the finite zero place. Now Y_0 has a zero place, where the numerator is zero:

$$z=-\frac{1}{T_r}(1-\sigma^2).$$

Fig. 7 shows the root-locus curves for the typical cases in the complex plane. The curves starting from poles p_1 and p_2 run to the infinite along asymptotes with slope $\pm\pi/2$. The intersection of the asymptotes with the real axis is in the geometrical centre of gravity of the poles and zero places, which is

$$a^*=-\frac{1}{2T_r}(1+\sigma^2).$$

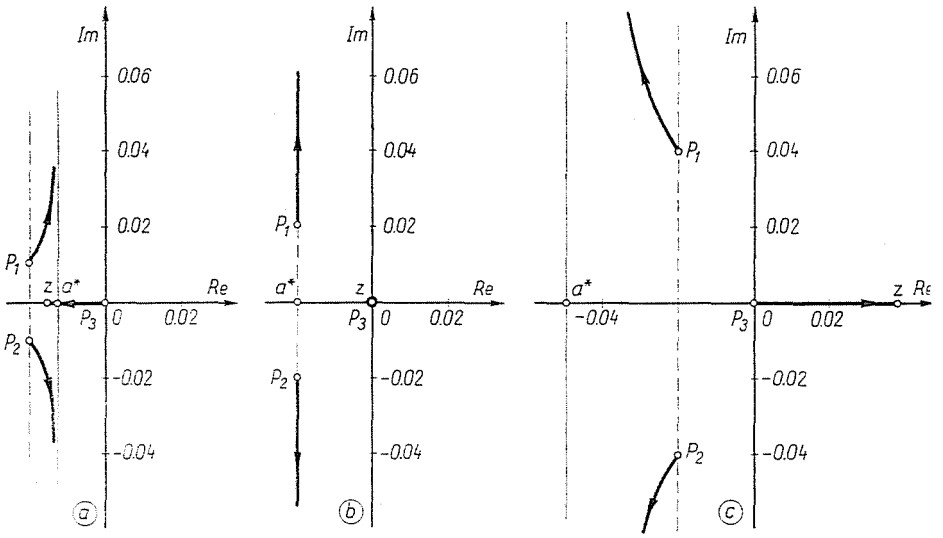

Fig. 7. Root-loci of the uncontrolled system: a) stable case, b) limitation case, c) unstable case

From this it can be seen that the asymptotes always lie in the left half-plane, and as according to (16) the same holds for the poles $p_{1,2}$, it follows that no instability can result from the conjugate complex root pairs.

Instability can result only from the third root-locus lying on the real axis starting from pole p_3 and running into zero place z. This is the locus of the real root of the third order characteristic equation of the closed system. Part a) of Fig. 7 shows a stable and c) an unstable case; part b) shows the limitation case. Stability depends on the position of the zero place relative to the zero point, i.e. if $z<0$, the system is stable, otherwise it is unstable. From the series of Fig. 7 it is evident that the reversal of the root will occur when point z passes the zero point, that is at the boundary of

stability $z=p_3=0$. From this, using the foregoing expression of z, the condition of stability is:

$$|\sigma|<1 \tag{17}$$

Therefore the area of stability for the uncontrolled drive will extend from the no-load point to the breakdown point, both in motor and generator operations. This area is practically very narrow, not only because the slip at maximum torque is smaller by one order than would be in the case of the supply with "Voltage Source", but mainly because this narrow area cannot be exploited perfectly on account of the airgap flux path being saturated.

For a better understanding Fig. 8 shows the torque-slip characteristics of the motor to be discussed later, whose parameters are constant stator currents. The line $\Psi_r=$const. is a path belonging to the constant rotorflux — which is equal to the no-

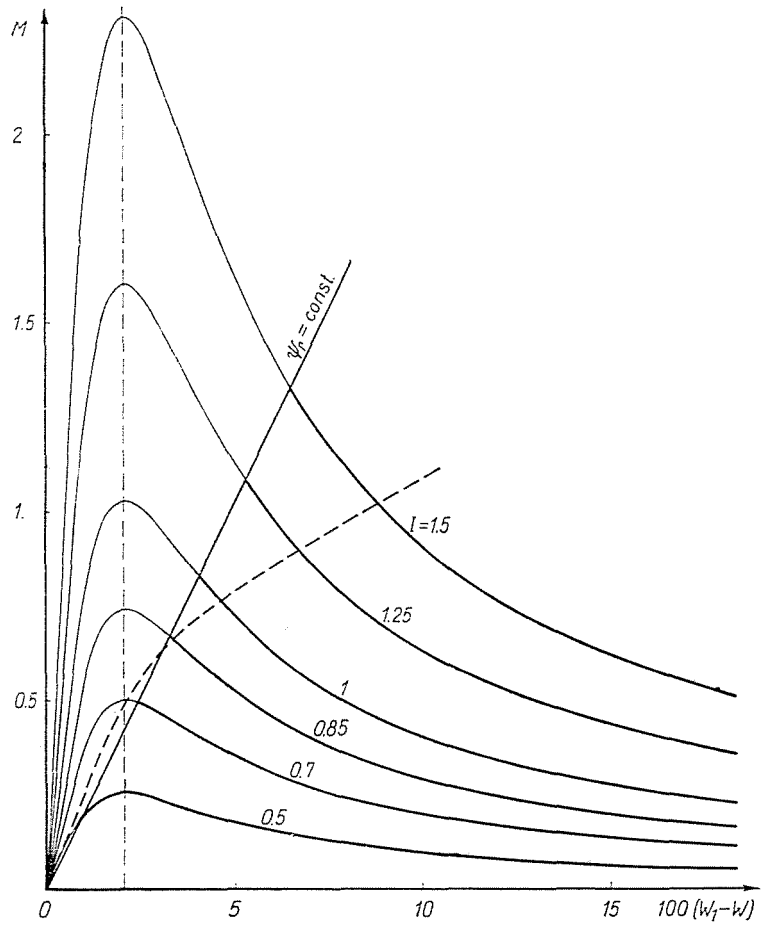

Fig. 8. Static torque-slip characteristics

load value. (The characteristic belonging to the constant airgap flux practically coincides with it.) The characteristics lying left from the line belong to smaller, and those at the right part to greater rotorfluxes than the mentioned one. As a flux considerably higher than the no-load flux cannot be permitted because of saturation, the operating points can be situated practically only around the line $\Psi_r = \text{const.}$, or to the right from it. This means that the drive — as seen from the Figure — has practically to work always in the unstable area, except for a closer vicinity of the no-load point.

The instability of the uncontrolled system is a known fact, which can be proved from the foregoing with the aid of the static characteristics. Really, the condition $z = p_3 = 0$ is identical with $Y_{mw} = 0$ and $s = 0$; so the condition $Y_{mw} = m/w = \partial M/\partial W = 0$ gives the breakdown point of the static mechanical characteristics, and thus the above condition is in fact the static stability criterion. As could be seen, the electromagnetic storages of the rotor — which are responsible for the conjugate complex root pair $p_{1,2}$ — do not cause instability. Our method cannot detect other possible instabilities of purely electrical type — which can be caused, for instance, by the inverter, — as all the energy storages have been neglected in the stator circuit.

However, we should like to point out, that the primary, decisive reason of the uncontrolled systems instability is of mechanical type, which is in connection with the instability of the static mechanical characteristics as described previously. If this reason is eliminated by means of appropriate feedback, then the stability of the system will be assured against other possible reasons as well.

5. Current control

Current control is the simplest way of stabilizing the system. Fig. 9 shows the schematic, well known solution of this in accordance with [1]. Of course, the solution comprises the speed (frequency) control, too, and this gives for the current control — with adequate limitation — the part of the current reference that is a function of the load. According to the block diagram of Fig. 9 the synchronous speed determined by the speed control:

$$W_1 = W + k_w(W_R - W) \tag{18a}$$

where W_R is the speed reference, k_w is the gain coefficient of the error-amplifier, whose magnitude depends on the permitted static speed error. From (18a) it can be seen, that $k_w = 1 + K$, where K is the static gain coefficient of the opened speed-control loop.

The reference of the current control consists of two parts: a constant part corresponding to the no-load current, and a changing part, which is dependent on the load. The latter part is proportional to the speed error $k_w(W_R - W) = W_1 - W$, thus it is a current control subordinated to the speed control.

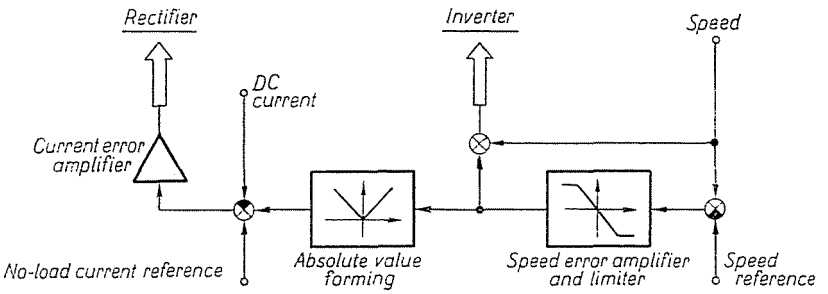

Fig. 9. Schematic of a simple current and speed control

No considerable error will result from assuming the current control to be ideal, i.e. its error to be zero. With this, the following fundamental expression holds for the current control:

$$I = I_0 + k_c(W_1 - W) \tag{19a}$$

where I_0 is the no-load stator current, and k_c is the gain coefficient of the reference dependent on the load, as interpreted according to (19a). Forming the absolute value in (19a) is simple, as the sign of k_c is always taken to be equal with the sign of $(W_1 - W)$. As can be seen very clearly from (19a), the value of coefficient k_c depends on at which rotor frequency the rated current should exist. Since, to avoid saturation of the magnetic path of the main fluxes and to utilize the motor in torque, it is desirable to get the rated current around the rated rotor frequency, there is obviously no great choice for k_c.

Changing over to small deviations, in accordance with (2), we get from (18a):

$$\varphi = \frac{k_w w_R - (k_w - 1)w}{s} . \tag{18b}$$

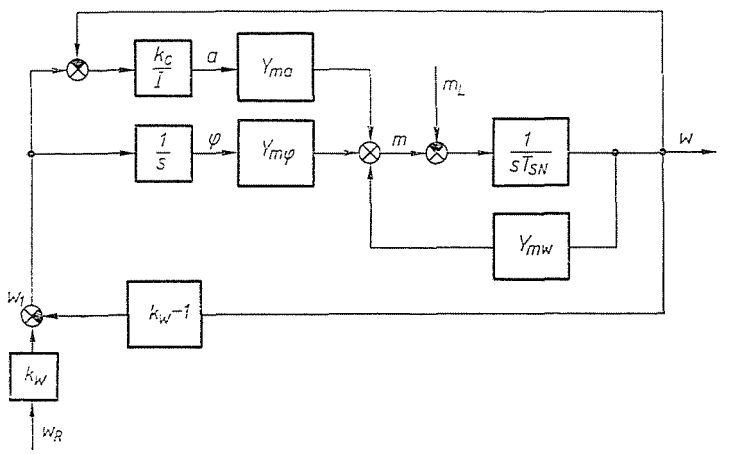

Fig. 10. Block diagram of the system shown in Fig. 9

From (19a) the relative value of the current amplitude is:

$$a=\frac{k_c}{I}(w_1-w)=\frac{k_c}{I}k_w(w_R-w), \tag{19b}$$

as $I_0=$const. at a given position of the control.

The block diagram of the controlled drive is shown in Fig. 10 which was derived from the fundamental block diagram of Fig. 6, completed by the foregoing equations. Using (14) and (18b)–(19b) this can be reduced to the simple form shown in Fig. 11. The transfer functions here are:

$$Y_{mw_R}=\left[\frac{m}{w_R}\right]_{w=0}=\frac{k_c k_w}{I}Y_{ma}+\frac{k_w}{s}Y_{m\varphi} \tag{20}$$

$$Y^*_{mw}=\left[\frac{m}{w}\right]_{wR=0}=Y_{mw}-\frac{k_c k_w}{I}Y_{ma}-\frac{k_w-1}{s}Y_{m\varphi}. \tag{21}$$

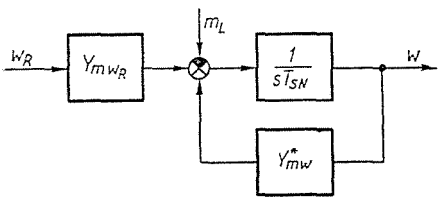

Fig. 11. Reduced block diagram

Knowing these, the dynamical performance of the controlled system can be studied. For sake of simplicity let us again examine the effect of the load torque, so let $w_R=0$, and let the question of stability be considered. Here, too, it is most practical to examine stability by using the characteristic roots of the closed loop system. In the case examined, the transfer function of the closed loop system is:

$$Y=\frac{w}{m_L}=-\frac{\frac{1}{sT_{SN}}}{1-\frac{1}{sT_{SN}}Y^*_{mw}}=-\frac{1}{sT_{SN}-Y^*_{mw}}.$$

By substituting (21) and (15a, b, c) and after simplifications, the following final result is obtained for the characteristic equation:

$$y^3+(q_1-1)y^2+(q_2+\sigma^2)y+q_1(1+2\sigma^2)-(q_2+1)\sigma^2=0 \tag{22}$$

where for simplicity

$$y=1+sT_r$$

$$q_1=k_c k_w\frac{M}{I}\frac{T_r}{T_{SN}}$$

$$q_2=k_w\frac{\Psi^{*2}_r}{L_s-L'_s}\frac{T_r^2}{T_{SN}}.$$

When the coefficients k_c and k_w have been chosen, the roots of the characteristic equation will be obtained by solving (22). So the roots and root loci can be considered in the whole loading interval. In the following, to illustrate the quantitative relations, we use the parameters of an experimental drive under construction:

380/220 V, 12/20.8 A, 50 c/s, 5.5 kW, 1,445 rpm.

Further parameters in the p.u. system are: $L_s=L_r=2.22$, $L'_s=0.161$, $R_r=0.045$ and with these $I_0=0.45$, $T_r=49.33$, and finally $T_{SN}=61$ with the connected masses.

The rated slip of the motor is 3.66%, this is really the static error in the rated point without speed control. If we want to reduce this to 0.25%, then, in accordance with (18a), a gain coefficient $k_w=3.66/0.25\approx 15$ is required.

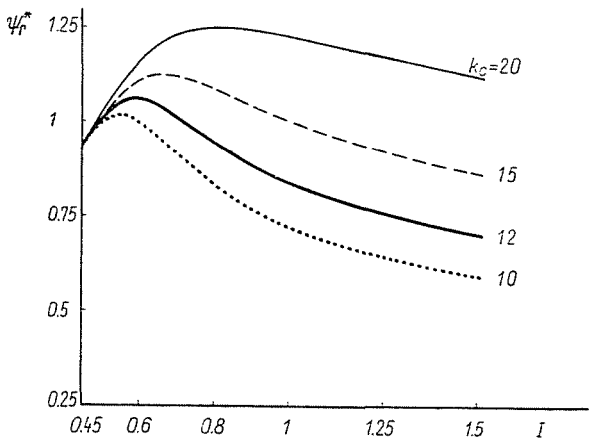

Fig. 12. The rotor flux as a function of the stator current in the case of a simple current control

With the current control assume that — as previously mentioned — it should regulate the rated current at rated rotor frequency. From (19a) follows that in our case a gain $k_c=(1-0.45)/0.0366\approx 15$ is necessary. The selection of k_c is, however, an important question of the current control, and so it is of interest to discuss it in more detail. In Fig. 12 — on the basis of (19a) and (5b) — the rotor flux was shown as a function of the stator current for the different values of k_c. It can be seen that the current control increases the rotor flux around the no-load point, and when the current increases, the rotor flux will decrease to an extent depending on k_c. From the point of view of the operational boundary of the inverter, some saturation is advantageous around no-load, but it can be seen that for the previously derived $k_c=15$ a significant saturation arises with greater loads, too; the rotor flux is 1 rel. unit even at rated current, instead of the value about 0.9 at normal saturation. The case $k_c=20$ cannot practically be accomplished, and in the other extreme case of $k_c=10$, the flux will decrease to an extent where the torque overloadability of the

motor will degrade. It can be seen, that the regulation of this current control is a difficult problem, and this method of control does not provide a good efficiency of the drive system.

Considering the foregoing, we chose $k_c=12$ instead of $k_c=15$. This seems to be the best compromise for our case. Now of course the rated current is not obtained at the rated rotor frequency, but at a rotor frequency higher by 15/12. As a consequence, the error of the rated speed will be 0.3% instead of 0.25. This can be compensated by taking k_w greater in the same proportion. As our drive is not sensitive in this respect, the error of 0.3% is permissible and so we have chosen the previous value $k_w=15$.

According to (7) and considering (19a) we have drawn the mechanical characteristic of the controlled drive in boken line in Fig. 8. An over-load of $I_{max}=1.5$ has been permitted to which $(W_1-W)_{max}=0.0875$ belongs; the limitation of the speed error must be regulated to this value. Fig. 8 shows that, from the view-point of speed control, the discussed control is not as advantageous as in the case of $\Psi_r=\text{const}$; the speed error without control increases rapidly with higher loads.

As all the necessary information is known, the roots of the characteristic equation (22) can be determined. First let only the effect of the current control be examined. Assume that the frequency is constant as prescribed from outside in an opened loop, so that the speed error is only formed for the current control. All of the equations are valid for this case, too, only $k_w=1$ must be assumed. This can be seen from (18b), considering that $w_R=0$. The root loci of the characteristic roots s are shown for this case in Fig. 13, in the per-unit system. As the root loci are symmetrically spaced around the real axis, therefore in the case of a complex root-pair it is sufficient to draw only one locus; we have used this method in the Figures detailed later.

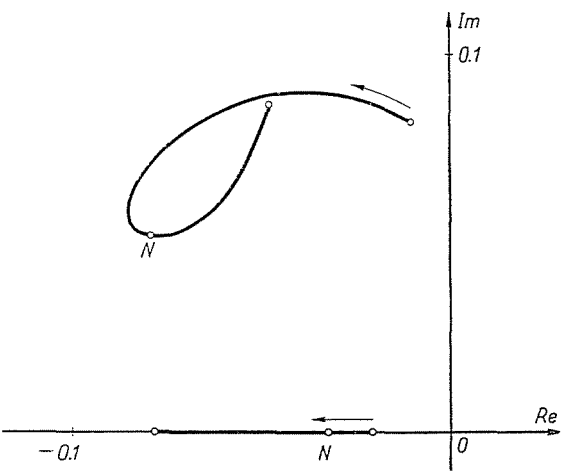

Fig. 13. Root-loci of the simple current control

The curves show the roots in the interval of currents from no-load to I_{max}. Arrows indicate the moving direction coming from the no-load point; the rated points are marked with N. As can be seen, the system becomes stable by the current control in the whole range of load. For example, in the rated point, the real root is -0.032 relative unit, that is $-0.032 \cdot 2\pi f_{1N} = -0.032 \cdot 314 \approx -10/s$, so the time constant of the aperiodic component is $1/10 = 0.1$ s. The complex pair of roots gives a damping component; the time constant of this is 0.04 s and the frequency of swinging 2.6 c/s in the rated point.

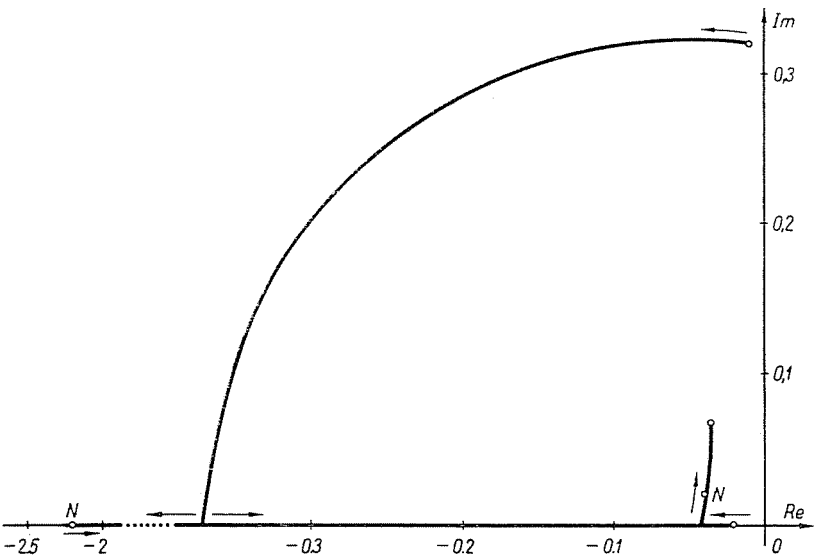

Fig. 14. Root-loci in the case of current and speed control

As the parameters of the induction motors of costumary design do not differ very much, and the previously discussed view-points determine the regulation of the current control in a relatively narrow interval, the general conclusion can be made, that the current control discussed is always capable of stabilizing the drive.

Fig. 14 shows the root-loci for a complete control, when speed control is also in operation. The Figure shows a favourable picture from the view-point of stability. The total interval of the real roots can be illustrated only by breaking the real axis and applying two different scales. The curve of large arc runs very fast into the real axis and in the tapping point $I = 0.515$. In the other tapping point, close to N, $I = 0.9$; all the three roots lying between the two points are real. So there is practically no pulsating component below the rated load; this refers to the fact that the operation of the drive is dynamically more uniform than in the case of a current control without speed control.

In our case the speed error reaches the limit-value at $I_{max} = 1.5$, and $(W_1 - W)_{max} = \text{const.}$ will be true, however large $(W_R - W)$ is. The current control,

which was supposed to be ideal will keep the current at the value $I_{max}=$const. and so $a=0$. On the other hand, for small deviations, due to the foregoing, $w_1=s\varphi=w$; therefore from (14) we get:

$$m=\left(Y_{mw}+\frac{1}{s}Y_{m\varphi}\right)w=0$$

which is not surprising as the rotorflux and therefore also the torque is constant, owing to the constant current. It follows that according to the block diagram of Fig. 10 the resultant transfer function in the discussed operational interval (e.g. at starting):

$$Y=\frac{w}{m_L}=-\frac{1}{sT_{SN}} \tag{23}$$

which means an integrating-type system.

6. Torque-angle Control

Another possibility for stabilizing the *CSI* drive is the so called torque-angle control. The basic idea in detail is found in [4], so we discuss it only to the extent necessary for the application of our method.

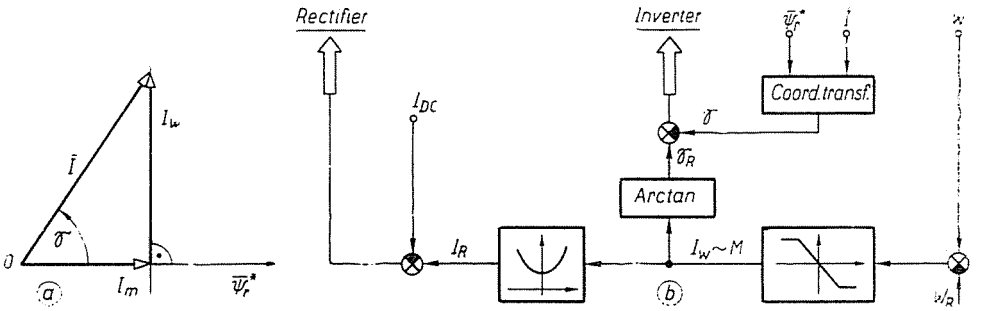

Fig. 15/a. Vector diagram in the case of torque-angle control
Fig. 15/b. Simplified schematic of torque-angle control

The torque of the induction motor is $M=\bar{\Psi}_r^* \times I=\Psi_r^* I \sin\gamma$, where γ is the angle between the vectors $\bar{\Psi}_r^*$ and I. If the rotorflux is controlled to be constant, then the torque will be proportional to $I \sin\gamma$. The current vector diagram of Fig. 15/a refers to this case. The constant rotorflux is produced by a constant magnetizing current I_m in phase with the flux; this current is actually the no-load current. When load is present, a perpendicular component $I_w=I\sin\gamma$ will be superposed on this component, and this will produce the torque proportional to it. The conditions are

similar to those of a separately excited d. c. machine, where the torque is similarly produced by the interaction of a constant armature flux and an armature current perpendicular to the flux. These conditions can be produced according to Fig. 15/a by providing a reference signal of $\gamma_R = \arctan(I_w/I_m)$ for the angle γ, and

$$I_R = \sqrt{I_m^2 + I_w^2}$$

for the current. A greatly simplified scheme of solution is shown in Fig. 15/b.

Let us choose the parameters of the control circuits such that the control keeps the no-load rotorflux constant, i.e. $I_m = I_0 = \text{const.}$, and therefore

$$\Psi_r^* = \Psi_{r0}^* = (L_s - L_s')I_0 = \text{const.}$$

It follows from (5b) that

$$I = I_0\sqrt{1+\sigma^2} \tag{24}$$

which, by substitution into (7), will give

$$M = (L_s - L_s')I_0^2\sigma. \tag{25}$$

In Fig. 8 the line of $\Psi_r = \text{const.}$ shows this characteristic with the previously given motor parameters. As can be seen, the static speed error without control is less with greater loads than in the case of the previously discussed control (see the curve in broken line). If for instance we want the speed error with control to be equal at the rated torque in both cases, then $k_w = 13$ will also be suitable instead of the previously shown value 15.

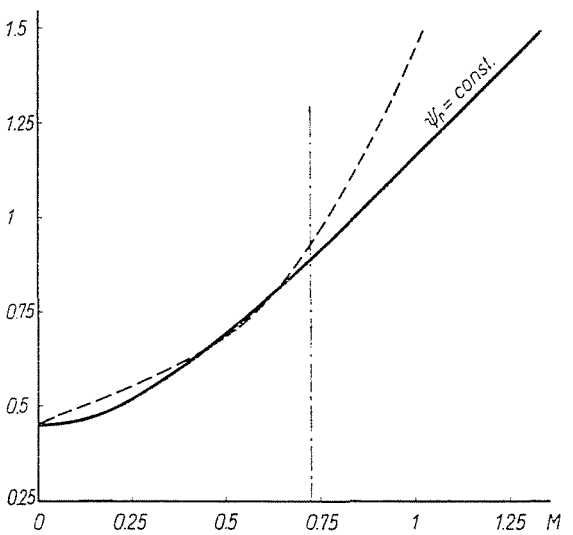

Fig. 16. Current-torque characteristics

By eliminating σ, from the above two formulas we get for the expressions of the $I(M)$ characteristic:

$$I=\sqrt{I_0^2+\frac{M^2}{(L_s-L_s)^2 I_0^2}} \tag{26}$$

This characteristic is shown in Fig. 16 with the indication of $\Psi_r=\text{const}$; the reference signal I_R of the current control must be formed accordingly. For comparison, this Figure shows also the characteristic $I(M)$ belonging to the previously discussed simple current control plotted in broken lines. It can be seen that, in spite of the fact that we tried to make the gain coefficient k_c optimal, the overloadability in torque is worse than in the case of torque-angle control.

Concerning the dynamic conditions, we obtain from (24) for the small deviation of the relative current amplitude:

$$a=\frac{1}{I}\frac{\partial I}{\partial \sigma}\Delta\sigma=\frac{1}{I}I_0 T_r\frac{\sigma}{\sqrt{1+\sigma^2}}(w_1-w).$$

Comparing this with (19b), it follows that the block diagram, the transfer functions and the characteristic equation evolved in the previous section can be used for analysing the torque-angle control, if for k_c the expression

$$k_c=I_0 T_r\frac{\sigma}{\sqrt{1+\sigma^2}} \tag{27}$$

is substituted, which is dependent on the operational-point. Solving the characteristic equation (22) in this way, we obtain the curves of the root-loci shown in Figs 17 and 18.

Fig. 17 refers to the case of $k_w=1$, i.e. to the system without speed control and Fig. 18 to the complete control. In this case we suppose the gain coefficient to be $k_w=11$, and then the static error will be the same with $I_{\max}=1.5$ as in the case of a

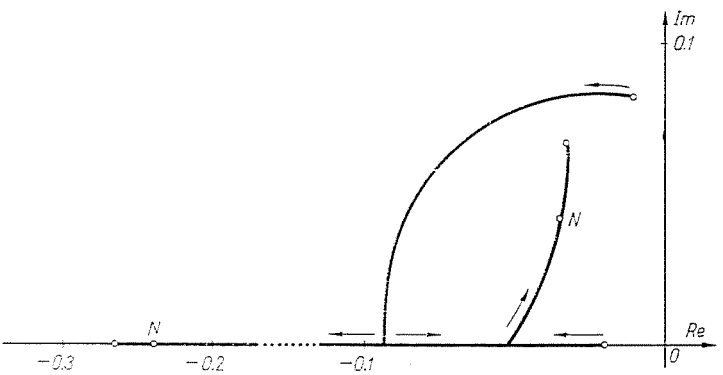

Fig. 17. Root-loci in the case of torque-angle control, without speed control

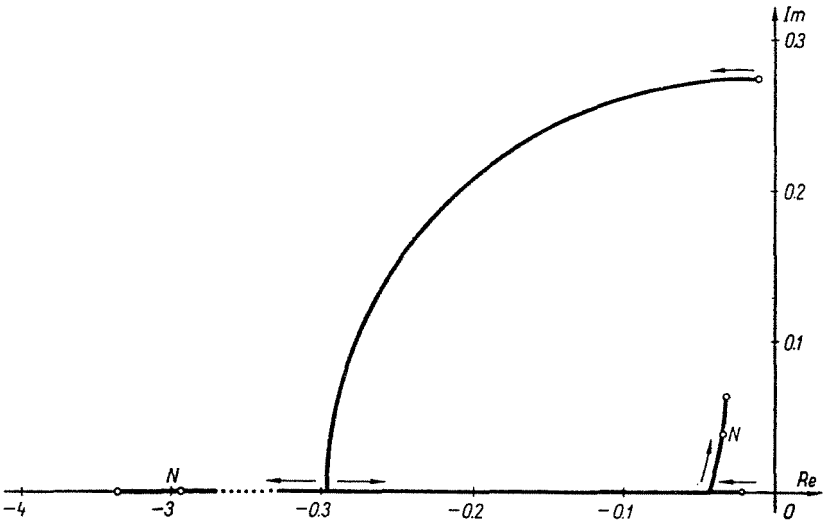

Fig. 18. Root-loci in the case of torque-angle control with speed control

simple current control. From a comparison of these curves with the root loci of Figs. 13 and 14, it can be seen that the two controlling methods discussed are equal and dynamically similar to each other from the view-point of stability. From other view-points the torque-angle control has some advantageous properties.

In the two examples discussed in the foregoing, we wanted to show the application of the simple dynamical investigating method presented in the paper. Of course, the method can be applied also for other controls possible in CSI drives. Transfer functions, frequency-loci or time functions of small deviations, etc., can be determined in the case of other signals, too.

Summary

A simplified analysis of the dynamic behaviour of induction motors fed by Current Source Inverters (CSI) is presented. The basic idea of the method is to approximate the theoretically rather complicated CSI by an ideal current source of fundamental harmonic. The approximation eliminates the two stator time constants. The induction motor has three energy storages in this simplified mathematical description valid, however, only for the fundamental harmonic. By using Park-vectors, the basic differential equations of the simplified system can easily be set up.

Linearizing at small deviations, transfer functions can be determined between the motor torque and various control signals by using the superposition theorem. If the transfer functions are known, a simple block diagram provides a means for studying the system by classical control theories frequency method, root-locus method, etc.). Stability criteria, for instance, can easily be derived both for open circuits and for feedback loops, and the control circuit parameters can also be estimated, etc. For the illustration of the described method the dynamic behaviour is shown for different ways of control.

References

1. PHILLIPS, K. P.: Current Source Converter for AC Motor Drives. IEEE Transactions, Vol. IA-8, No. 6, 1972, Nov.—Dec., pp. 679–683.
2. CORNELL, E. P.–LIPO, T. A.: Design of Controlled Current AC Drive Systems Using Transfer Function Techniques. IFAC Symposium on Control in Power Electronics and Electrical Drives, Düsseldorf, October 1974, Vol. 1, pp. 133–147.
3. RÁCZ, I.: Betrachtungen zu Oberwellenproblemen an Asynchronmotoren bei Stromrichterspeisung. Periodica Polytechnica, Vol 11, No. 1–2. 1967, pp. 29–57.
4. BLASCHKE, F.: Das Verfahren der Feldorientierung zur Regelung der Asynchronmaschine: Siemens Forschungs- und Entwicklungsberichte, 1/1972, pp. 184–193.
5. KOVÁCS, K. P.–RÁCZ, I.: Transiente Vorgänge in Wechselstrommaschinen. Verlag der Ungarischen Akademie der Wissenschaften, Budapest, 1959.
6. ANCKER, J.: Analysis and Simulation of an Induction Motor Drive Supplied from a Current Source Frequency Converter. Ph. D. Thesis, Stockholm, 1976.

Dr József LÁZÁR H–1521 Budapest